American Journal of Analytical Chemistry, 2015, 6, 631-643
Published Online June 2015 in SciRes. http://www.scirp.org/journal/ajac
http://dx.doi.org/10.4236/ajac.2015.67061

Hollow Fiber Supported Liquid Membrane for Separation and Recovery of $^{152+154}$Eu and ^{90}Sr from Aqueous Acidic Wastes

A. T. Kassem*, Y. T. Selim, N. El-Said

Hot Labs. and Waste Management Center, Atomic Energy Authority, Cairo, Egypt
Email: *amany.kassem00@gmail.com

Received 17 May 2015; accepted 27 June 2015; published 30 June 2015

Abstract

Separation and recovery of $^{152+154}$Eu and ^{90}Sr from radioactive waste using tracer concentration from active material from waste tank in the ET-RR1 Egypt via hollow fiber supported liquid membrane (HFSLM) were achieved. The Polypropylene was used as supporter to carrier 0.5M Cyanex301/kerosene (bis(2,4,4-trimethylpentyl)dithiophosphinic acid and 0.1MEDTA as stripping of $^{152+154}$Eu and ^{90}Sr ions from nitrate medium at pH ~3.6. The separation factor was found to be ~4 for $^{152+154}$Eu over ^{90}Sr. The aqueous feed of mass transfer coefficient (k_i) and the organic mass transfer coefficient (k_m) were calculated to be (1.52 and 4.5) × 10^{-2}cm/s, respectively. In addition, the mass transfer modeling was performed and the validity of the developed model from experimental data was found to join in well with the theoretical values when the Cyanex301 concentration is higher than 1% (v/v). The number of cycles evaluated for complete separation of $^{152+154}$Eu and ^{90}Sr is five cycles.

Keywords

Hollow Fiber Supported Liquid Membrane, Separation and Recovery, $^{152+154}$Eu and ^{90}Sr, EDTA (Stripping Phase)

1. Introduction

Overview and Background

Radionuclide contamination distributions and their impacts of relative to contamination sources are the primary

*Corresponding author.

How to cite this paper: Kassem, A.T., Selim, Y.T. and El-Said, N. (2015) Hollow Fiber Supported Liquid Membrane for Separation and Recovery of $^{152+154}$Eu and ^{90}Sr from Aqueous Acidic Wastes. *American Journal of Analytical Chemistry*, **6**, 631-643.
http://dx.doi.org/10.4236/ajac.2015.67061

focus and separation by a Novel technique as hollow fiber supported liquid membrane of this work. Although the wastewater samples which are present in the waste tank were found in assay of all radionuclide contamination, the number of radionuclide contamination in the ET-RR1 Egypt reactor zone is desirable. The technology used (passive gamma logging) allows only an assay of gamma-emitting radionuclides. The radionuclide contamination in the ET-RR1 reactor in Egypt zone can be considered to present both a short-term occupational exposure risk to operations workers and a long-term risk to the public and the environment. The types of possible risks depend on a variety of factors that are specific to each radionuclide, including the decay half-life of the nuclide, its mobility in the water and soil contamination (and ultimately in the groundwater), and its specific activity and/or biological toxicity [1]-[3]. Long-term human health risks arise primarily from a potential pathway where by an individual is exposed by ingesting contaminated groundwater and from a pathway involving direct exposure of an individual to contaminated sediment that is uncovered or otherwise brought to the surface in the distant future. There are some elements that have raised the risk of long-term waste tank. Many of the radionuclides that are in the original waste have a short half-life of the tank, however no longer detectable. Europium radionuclides in the tank wastes include the isotopes Eu-152 and Eu-154. Eu-154 originates from the activation of europium-153 (Eu-153), which is a fission product. Eu-154 is not as abundant in the irradiated fuel or the processing waste streams as Cs-137, but it is present in irradiated fuel at high enough concentrations that it contributes a significant amount to the total radiation flux from the fuel. Sr-90 is similar to Cs-137 because it is also a high-yield, long-lived fission product with a half-life of 29 years. Unlike Cs-137, Sr-90 decays with the emission [4] of a beta particle but no gamma-ray photons. Sr-90 decays to yttrium-90 (Y-90), which has a short half-life (64 hours), and to stable zirconium-90 (Zr-90). The beta particle emitted in the decay of Y-90 has a high energy (2.2 million-electron-volts [MeV]) and is usually associated with the parent radionuclide Sr-90. It is the second most abundant radionuclide in the tank waste material. In the high-heat and self-boiling tanks the decay of Sr-90 generates more heat than all other radionuclides combined [5]. This heat is the result of the release of high-energy beta particles from the decay of Y-90. Sr-90 is dissolved easily during the fuel dissolution process, the first stage of fuel rod processing, and it stays in solution throughout the separation process [6]. Consequently, Sr-90 is always a component in effluent waste products to highlight the state of separation of $^{152+154}$Eu and ^{90}Sr by hollow fiber supported liquid membrane.

2. Experimental

2.1. Apparatus

Hollow fiber supported liquid membrane, In A laboratory scale Celgard X-30 polypropylene fibers were used in the experiment. And its properties are listed in **Table 1**. Both pH of feed and stripping solutions were measured by B-417 HANA instrument. For equilibrium experiments a good shaker of the type SANKYO, a Centrifuge of the type UNIVERSAL with. a muffle furnace from LINDBERG and a special micropipette with disposable tips were used. Tri-Carb 1600 CA liquid scintillation analyzer was used for the determination of β-emission via liquid scintillation solution (Hionic fluxar). A model 800 A multichannel analyzer consisting of NaI (Ti) activated crystal flat type of 256 channels connected to an automatic scaler was used for counting the gamma activity. All chemicals were of A.R. grade and supplied by Merck. The HFSLM module was prepared using polypropylene micro-porous membrane lumens obtained $^{152+154}$Eu and ^{90}Sr from and (Shanghai Liquapure Filtration Co., Ltd**) [7]**, respectively. The $^{152+154}$Eu and ^{90}Sr tracer (1×10^{-3} moldm^{-3}) and initial volume activity of feed solutions about 1000 Bq·Cm^{-3} was purified by the usual dispersed emulsion membrane method.

2.1.1. Reaction Mechanism for Hollow Fiber Supported Liquid Membrane System

The HFSLM system consists of three phases those are feed phase, organic membrane phase and stripping phase. The aqueous feed solution was $^{152+154}$Eu and ^{90}Sr radioactive waste) and EDTA was used as stripping phase. The aqueous feed phase and stripping phase were in contact with the organic membrane phase. The extractant cyanex301 (bis(2,4-4,trimethylphenyl)-dithiophosphonic acid in kerosene) is filled in the membrane pores. The aqueous feed flows inside the tube and stripping solution flows in the shell of module. The flow between tube and shell sides is in counter current direction. The transport mechanism of $^{152+154}$Eu and ^{90}Sr are so called couple facilitated counter-transport, as shown **Figure 1** in Transport scheme of extraction and stripping in a liquid membrane process using cyanex301 as a carrier.

$^{152+154}$Eu and ^{90}Sr diffuses from the feed phase to the feed-membrane phase interface $^{152+154}$Eu and ^{90}Sr. The

extraction of $^{152+154}$Eu with cyanex301/kerosene can be expressed.

$$^{152+154}\mathrm{Eu},^{90}\mathrm{Sr}\left(\mathrm{feed}\right)+2\left(\mathrm{HR}\right)_{3\mathrm{org}}\leftrightarrow {}^{152+154}\mathrm{Eu},^{90}\mathrm{SrR}_2\left(\mathrm{HR}\right)_{2\mathrm{org}}+3\mathrm{H}^+ \tag{1}$$

where cyanex301 as soft donor ligand and selectivity for trivalent complex, high Viscosity at 25˚C so that the $^{152+154}$Eu and ^{90}Sr are(complexes) with a carrier diffusion through the membrane phase from interface feed phase to interface membrane phase, and the metal complex produced pervious step reacts with hydronium ions ($3H^+$) at the membrane stripping phase by 0.1 M EDTA as stripping phase and the carrier recycle from interface Feed phase ↔ Membrane phase and return to from Membrane ↔ feed. Calculate percentage of extraction and stripping phase from Equation (2).

$$\%\mathrm{Extraction}=\frac{C_{\mathrm{feed}}-C_{\mathrm{feed,out}}}{C_{\mathrm{feed,in}}}\times 100 \tag{2}$$

$$\%\mathrm{Stripping}=\frac{C_{\mathrm{s,out}}}{C_{\mathrm{feed,in}}}\times 100 \tag{3}$$

$C_{\mathrm{s,out}}/C_{\mathrm{feed,in}}$ Concentration of stripping out let and concentration in feed inlet.

2.1.2. Characterization of Hollow Fiber Module

The facilities of transport mechanisms through the hollow fiber module **Figure 1**, used widely for the separation applications and the selectivity is controlled by both the extraction of radioactive waste by using hollow fiber module **Table 1** Shows the properties of the hollow fiber module (Shanghai Liquapure Filtration Co., Ltd). The extraction and stripping (back-extraction) equilibrium at the interfaces and the kinetics And transferred complex species under a non-equilibrium mass-transfer process. The single module operation is shown in **Figure 2** (SEM-polypropylene HFSLM). **Figure 3** shows cross-section in HFSLM. **Figure 4(a)** Experimental set up of the hollow fiber liquid membrane system, **Figure 4(b)** shows schematic diagram of HFSLM system, Where Cyanex 301 is used as the carrier diluted in kerosene (fluka) and EDTA was used as received phase for hollow fiber module through circulation into shell and tube for 90 min. After that the feed solution entered the tube side whereas the stripping solution with EDTA entered shell side but it was in counter current direction. The $^{152+154}$Eu and ^{90}Sr tracer radioactive in the nitrate medium solution were moved across the liquid membrane to stripping phase and were accumulated in the stripping phase. The concentrations of $^{152+154}$Eu and ^{90}Sr ions in sample from the feed and the stripping solutions were analyzed by multichannel to determine the percentage of extraction and stripping. The extractant of cyanex301 (bis(2,4-4,trimethylphenyl)-dithiophosphonic acid. were obtained from Merck, Where cyanex301 as soft donor ligands so selective trivalent complex The aqueous solution was provided from tracer radioactive waste dissolved in 0.1 M HNO_3. All other chemicals such as nitric acid and kerosene were obtained from sigma Aldrich. The feed phase was not diluted but only adjusted pH by nitric acid. The receiving [8]-[16] or striping phase was prepared from the stock solution by dilution with distilled water to the desired concentration. The organic phase is used as a carrier and dissolved in kerosene.

2.1.3. Extraction of Equilibrium Constant and Distribution Ratio

Study the K_{ex} as extraction constant for X = $^{152+154}$Eu and ^{90}Sr ion that extracted by Cyanex301/kerosene can be calculated using [17].

$$K_{ex}=\frac{\left[\mathrm{XR}_2\left(\mathrm{HR}\right)_2\right]\left[\mathrm{H}^+\right]^3}{\left[\mathrm{X}\right]\left[\mathrm{HR}\right]_2\right]^3} \tag{4}$$

And the distribution ratio (D) for X given by

$$D=\frac{\left[\mathrm{XR}_2\left(\mathrm{HR}\right)_2\right]}{\left[\mathrm{X}^{3+}\right]} \tag{5}$$

According to the distribution ratio equations as a function of extraction equilibrium constants

$$D=\frac{K_{ex}\left[\left[\mathrm{HR}\right]_2\right]^2}{\left[\mathrm{H}^+\right]^3} \tag{6}$$

Table 1. Properties of the hollow fiber module.

Properties	Description
Materials	polypropylene
Fiber i.d	240 µm
Fiber o.d	300 µm
Pore Size	0.05 µm
porosity	30%
Contact area	1.39 m^2
A/unit V	29.3 cm^2/Cm^2
Molecular diameters	6.3 cm
Module diameter	20.3 cm

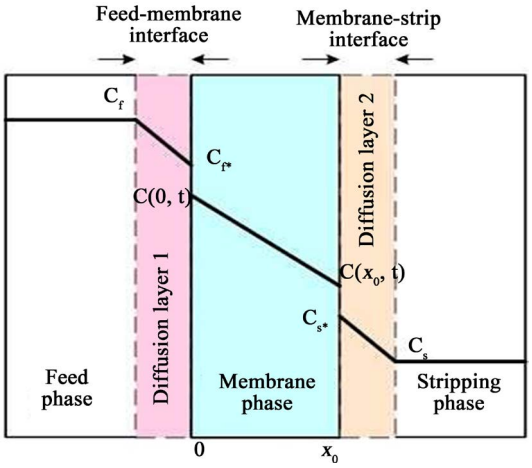

Figure 1. Transport scheme of extraction and stripping in a liquid membrane process using cyanex301 as a carrier/kerosene [Huang's diffusion model].

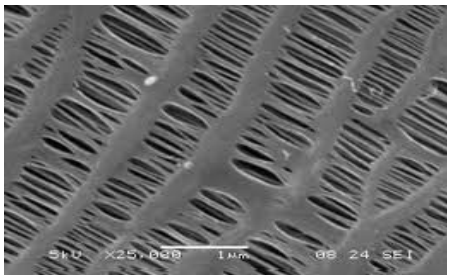

Figure 2. SEM-polypropylene HFSLM.

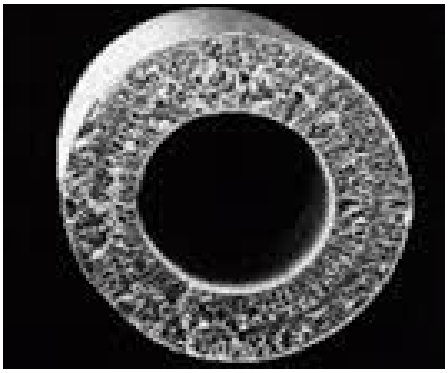

Figure 3. Cross-section in HFSLM.

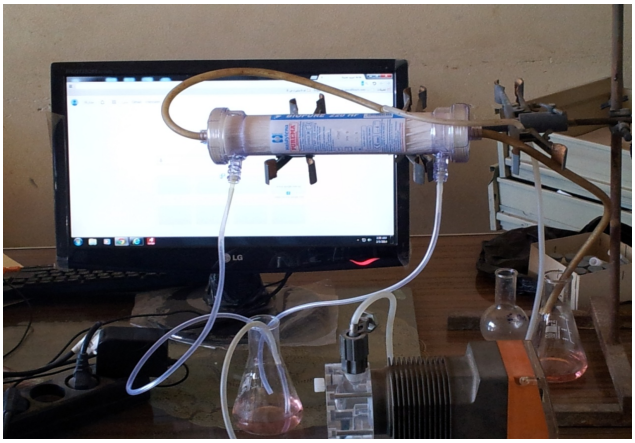

(a)

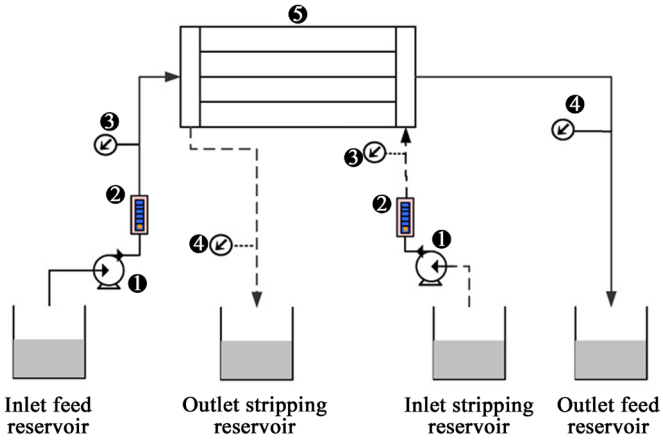

(b)

Figure 4. (a) Experimental set up of the hollow fiber liquid membrane system. (b) Schematic diagram of HFSLM system: (1) feed; (2) glass-body; (3) fiber; (4) pump; (5) strippant.

2.1.4. Evaluation the Permeability of Hollow Fiber Membrane [17]

Evaluation the permeability of hollow fiber membrane of radioactive waste in the HNO_3 (1 M). Hollow fiber is placed in a solution within a very large glass tube. The hollow fiber is 20.3 cm in length, with a diameter of 6300 microns. Liquid flow rate contain dissolved permeable through the hollow fiber is 1 ml/min. Found that the solute concentration and permeability out of the hollow fiber is 10% of the concentration of this solution when entering the hollow fiber. Evalution the permeability of the hollow fiber membrane for this we will consider a simplified model for solute transport in the hollow fiber. We assume that the flow rate in the shell space is much higher than that of the fiber so that the solute concentration in the shell space is zero and the resistance to the solute within the fiber is negligible so that $K_0 \approx P_m$. The steady state solute balance on the control volume $\pi rc^2 \Delta Z$ gives.

$$V\pi rf^2 C\Big|_z - V\pi rf^2 C\Big|_{z+\Delta z} = -2\pi rc\Delta z k_0 (C-0) \tag{7}$$

where K_0 is the overall mass transfer coefficient between the solute in the hollow fiber and the solute in the shell space next to the hollow fiber wall, and C is the solute concentration in the fiber. The solute concentration in the surrounding shell space is zero. The overall mass transfer coefficient is related to the film mass transfer coefficient and the permeability by the expression.

$$\frac{1}{k_0} = \frac{1}{k_m} + \frac{1}{P_m} \tag{8}$$

where $\frac{1}{k_0}, \frac{1}{k_m}$ and $\frac{1}{P_m}$ the total mass transfer resistance of solute from the fiber to the outside surface of the fiber, the mass transfer resistance in the fiber side, and the mass transfer resistance through the fiber wall, respectively [18]. Since $\frac{1}{k_m} \ll \frac{1}{P_m}$.

2.1.5. Determination of Mass Transfer in HFSLM

Determination of Mass transfer in HFSLM and the mass diffusion of $^{152+154}$Eu/^{90}Sr ions across immiscible liquid membrane phase from feed phase to the stripping phase. The direction of mass transfer depends on the driving force across the liquid membrane. The driving force can be the concentration gradient of $^{152+154}$Eu/^{90}Sr concentration/aqueous pH or H^+ concentration for the uphill transport in the case of the coupled facilitated transport as discussed earlier.

2.1.6. Mass Transfer Modeling

Mass transfer modeling through of the HFSLM modules [18]-[20] for recovery-concentration of $^{152+154}$Eu and ^{90}Sr using permeability coefficient $^{152+154}$Eu and ^{90}Sr centers on three mass transfer resistances. First occurs in the liquid following through the hollow fiber cavity. Second corresponds to the $^{152+154}$Eu and ^{90}Sr-Carrier and stripping phase diffusion across the liquid membrane immobilized on the porous wall of the fiber outside. The reciprocal of the overall permeability coefficient is given as below.

$$\frac{1}{P_X} = \frac{1}{K_i} + \frac{r_i}{r_{im}}\frac{1}{P_m} + \frac{r_i}{r_0}\frac{1}{K_s} \tag{9}$$

Where r_{lm} is the hollow fiber mean radius(cm), K_i and K_s the aqueous feed and stripping mass transfer coefficient in tube and shell side, respectively, and P_m the membrane permeability ,which is related to the partition coefficient of $^{152+154}$Eu and ^{90}Sr (D_r) with cyanex301 by

$$P_m = D_r K_m = K_{ex}\left[\mathrm{NO_3^-}\right]^4 \left[\mathrm{Cyanex301}\right]_{\mathrm{org}}^2 K_m \tag{10}$$

where K_m is the membrane mass transfer coefficient which is defined as

$$D_r = \frac{\mathrm{X(NO_3)_4} \cdot 2\left[\mathrm{Cyanex301}\right]_{\mathrm{org}}}{\left[\mathrm{X^{3+}}\right]} \tag{11}$$

X = $^{152+154}$Eu and ^{90}Sr

Introducing Equation (10) in Equation (11) gives P $^{152+154}$Eu & ^{90}Sr

$$P_x = \frac{S_P r_i \nu_f}{2\pi r_i^2 L N \nu_f - S_P L \varepsilon} \tag{12}$$

When the reaction is instantaneous at the stripping phase side, the contribution of the outer aqueous phase resistance is removed from Equation (9) and P $^{152+154}$Eu and ^{90}Sr is determined from

$$\frac{1}{P_X} = \frac{1}{K_i} + \frac{r_i}{r_{im} K_m K_{ex}} \frac{1}{\left[\mathrm{NO_3^-}\right]^4 \left[\mathrm{Cyanex301}\right]_{\mathrm{org}}^2} \tag{13}$$

2.1.7. Distribution Ratio for Liquid-Liquid Extraction

The distribution ratio for liquid-liquid extraction [19] in the hollow fiber supported liquid membrane measurement at equilibrium state. The volumes of $^{152+154}$Eu and ^{90}Sr at 1 ml tracer in nitric acid of desired molarity for cyanex301 from Equation (14).

$$\%E = 100 D_M \Big/ \left[D_M + \frac{V_w}{V_0} \right] \tag{14}$$

The distribution ratio (D_M) for $^{152+154}$Eu and ^{90}Sr is defined as the ratio of $^{152+154}$Eu/^{90}Sr concentration in the organic phase and aqueous phase. **Table 2** shown the calculate of HNO_3 concentration (1 M) and $K_{cons.} \times 10^{-8}$ (s^{-1}) respectively. After 2 hours.

2.1.8. Permeability Coefficient

The permeability coefficient (P), fast interfacial reactions [19], and the distribution of $^{152+154}$Eu and ^{90}Sr between the feed and membrane phase were calculated to be higher than those between the membrane and stripping phase. The Equation (14) for determining the permeability coefficient was expressed by *Sawicki*: The facillated of other simulated radioactive elements from water samples taken from Egyptian EET-R1 reactor and found there are elements such as cesium-137 and cobalt-60, iron-55, chromium-51 and other elements as possible to simulation in aqueous solution. But all of these elements have been taken into account where already moved to inside the hollow fiber supported liquid membrane was measured elements after almost 2 - 3 hours and measured by Multi-channel gamma radiation and using carrier cyanex301/keroseme 96.8%. In kerosene at pH ~3.6 has been moved $^{152+154}$Eu just inside the Hollow fiber supported liquid membrane and ^{90}Sr raffinate in the cerrier.

2.1.9. Diffusion of Membrane

The effective of diffusion coefficient [21]-[23] (D_{eff}) of $^{152+154}$Eu and ^{90}Sr extractant complex through the organic membrane phase were determined through mathematical modeling. Effective diffusion coefficient (D_{eff}) for the solute in the immobilized organic liquid membrane can be defined as follow:

$$D_{eff} = K_m t_m \tau \tag{15}$$

The permeation of a metal species through a hollow fiber SLM module in a recycling mode can be expressed in terms of the permeability coefficient, P^*, described by the following Equation [15]:

$$\ln\left(\frac{C}{C_0}\right) = \frac{AP^*(\phi+1)t}{V\phi} \tag{16}$$

where A is the total internal area of the hollow fiber module, V the total volume of the feed solution and C_0 in the concentration of metal species solution at time zero. Study the parameter for hollow fiber membrane containing N fiber is

$$\phi = QT/PLNR \tag{17}$$

where QT is the total flow rate of the feed solution, P the permeability, L the length of the fiber, N the number of the fibers and R is the internal radius of the fiber.

3. Result and Discussion

3.1. Effect of Carrier Concentration on the Permeability

Figure 5 and **Figure 6** Show that the permeation coefficient for $^{152+154}$Eu and ^{90}Sr was increased with carrier concentration up to 90% for $^{152+154}$Eu and remained constant up to 45% for ^{90}Sr there after 2 hr, it was observed to be decreased. This may be due to the increased viscosity at higher concentration of carrier, which in turn lowers the transport of metal ion .Thus 60% cyanex301 was selected as the optimum carrier concentration to carry out further experiments to evaluate different parameters where cyanex301 [bis(2,4-4-trimethylphenyl)-dithiophoshonic acid and the complex as soft donor ligands, and selective trivalent complex such as $^{152+154}$Eu.

3.2. Effect of Flow Rate

Figure 7 Illustrated the percentages of extraction and stripping as a function of volumetric flow rate. The feed solution flows in the tube and the stripping solution flows in the shell as the counter current direction. And the optimization between permeability coefficient, EDTA stripping plase and flow rates (−100 - 100) m/s in HFSLM. At 25˚C. The volumetric flow rates were studied at −100 at 100 mL/min under the condition of Cyanex301, 0.1 mol/L, 2.5 mol/L EDTA as a stripping solution, and operation time 60 min. Results of $^{152+154}$Eu and ^{90}Sr transport from medium active acidic waste (feed solution composition through HFSLM consisting of 30% Cyanex301/n kerosene using 0.1 M in feed solution and EDTA as stripping solution, at pH ~1.5 - 4.5 in recy-

Table 2. The calculate of HNO_3 concentration (1 M) and $K_{cons.} \times 10^{-8}$ (s^{-1}) respectively. After 2 hours.

D_M	$K_{cons.} \times 10^{-8}$ (s^{-1})
0.01	4.38
0.05	4.42
0.1	6
0.2	4.7
0.35	4.9
0.45	5.1
0.5	5.2
0.7	5.35
0.75	5.84

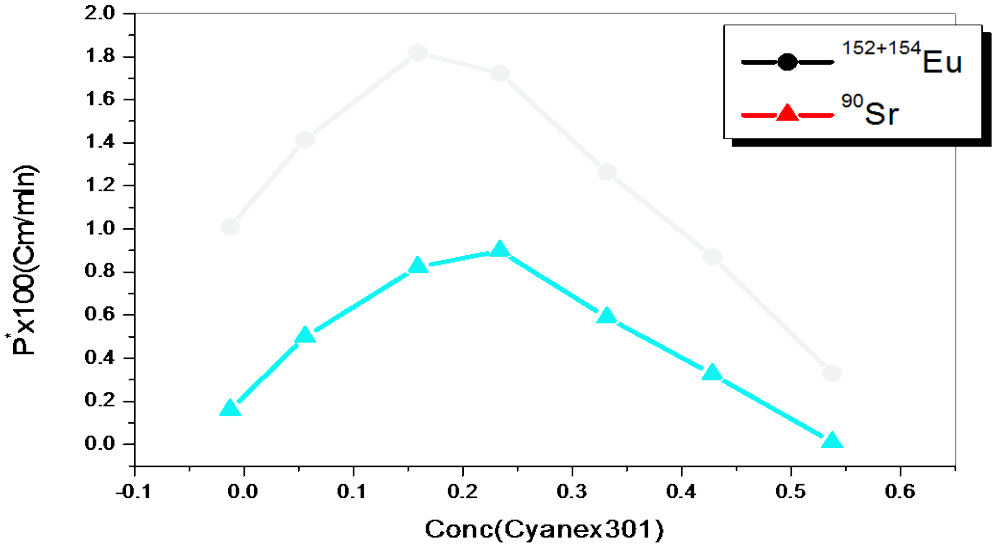

Figure 5. Permeability of $^{152+154}$Eu & ^{90}Sr as carrier concentration, at pH = 3.8.

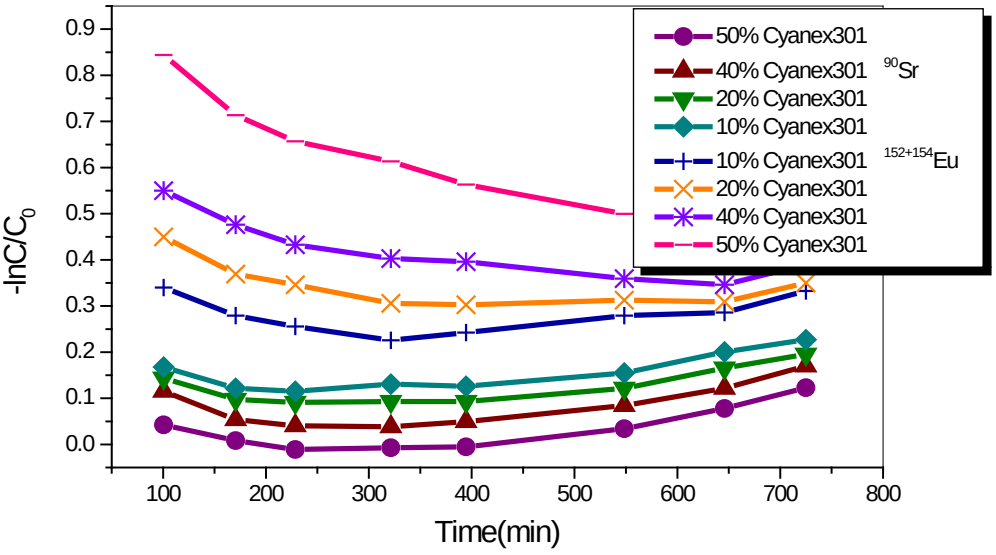

Figure 6. Effect of different concentration for cyanex301/kerosene.

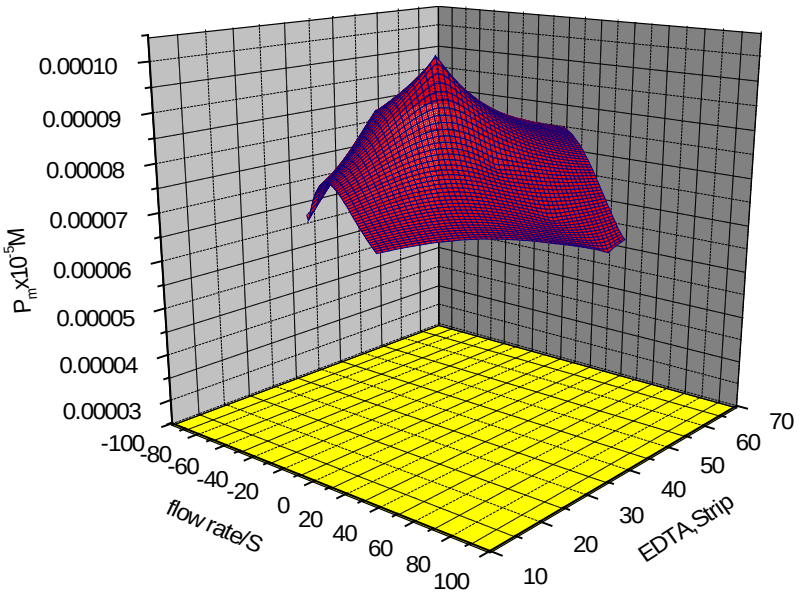

Figure 7. Optomization between P × 10^{-8}, EDTA stripping plase at 25(o)C and flow rates (−100 - 100) m/s in HFSLM.

cling mode. The percentage of $^{152+154}$Eu and ^{90}Sr transport versus time in strip and feed is depicted. The $^{152+154}$Eu and ^{90}Sr concentration in the feed decreased with time and the concentration in the stripping solution continuosly increase with time. After 1 h, the permeation of $^{152+154}$Eu and ^{90}Sr from the source phase was around 50% and to 1 ml·min^{-1}. Whereas the $^{152+154}$Eu transport from source phase was more than 65% and in strip phase was around 50% when flow rate of feed was increased to 3 ml·min^{-1}·s the permeation of $^{152+154}$Eu with *i* flow rate (1 ml·min^{-1}). High flow rate results in more linear flow velocity of feed which in turn give more transport of $^{152+154}$Eu from membrane phase to strip phase as increased flow rate and indicated that higher flow rate (3 ml·min^{-1}) was more linear compared to low flow rate.

3.3. Effect of Carrier

Cyanex 301/kerosene concentration on $^{152+154}$Eu and ^{90}Sr transport was also investigated. Experimental conditions were established as organic phase with various concentrations of Cyanex301 in the organic diluent, and feed concentration of 0.030 g/l $^{152+154}$Eu and ^{90}Sr at pH 3.8 ± 0.05. Results are shown in **Figure 8**, the mass transfer coefficient was seen to increase with Cyanex 301 concentration of up 25% v/v and the transport rate should be therefore limited by diffusion[23] through the aqueous film on the feed side of membrane in this region.

3.4. Effect of the Carrier on Permeability

Effect of The results concerning transport of $^{152+154}$Eu and ^{90}Sr from a feed phase containing metal ion concentration 10^{-5} to 10^{-4} M on transport of $^{152+154}$Eu and ^{90}Sr was investigated. The flux for two different concentration of metal ion was calculated from slope analysis technique **Figure 9**. The permeability coefficient as 3.25 × 10^{-5} Predicted) and 3.98 × 10^{-5} (experimental). Flux was found to be 32.56 L/m^2·h. The higher $^{152+154}$Eu concentration gradient between the aqueous feed phase to stripping phase across the liquid membrane, which enhances the transport of $^{152+154}$Eu ion. This initial increase in flux versus $^{152+154}$Eu is in accord with the expected trend since the flux of a cation varies with $^{152+154}$Eu following the relationship.

$$J_M = A\left[\frac{T}{\eta}\right]\left[\mathrm{NO_3^-}\right]_{aq}^{\eta}\left[\mathrm{Cyanex301}\right]_{\mathrm{org}}^{\eta}\left[\mathrm{X_{Eu,Sr}}\right]. \quad (18)$$

where *T*, η, $[\mathrm{Cyanex301}]_{\mathrm{org}}[\mathrm{X_{Eu,Sr}}]$ denote the absolute temperature, viscosity of the membrane phase. Cyanex concentration in the membrane (organic) phase, and concentration of $^{152+154}$Eu in the feed respectively.

In and equation $D_{eff} = K_m t_m \Gamma$. The slope of the straight line in **Figure 10** and this equation in kerosene is bound to the metal. The calculated value of membrane mass transfer coefficient (K_m) was found to be 5.02 ×

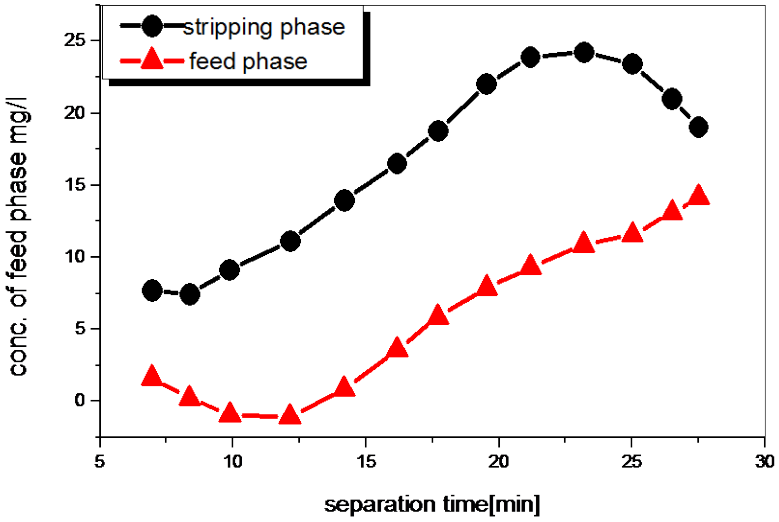

Figure 8. Concentration of \+$^{152+154}$Eu and ^{90}Sr against separation time (pH of feed solution 3.8.).

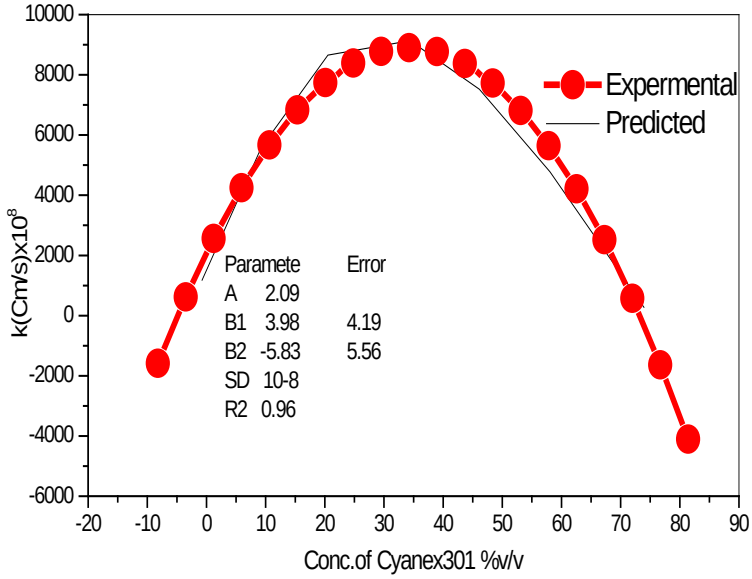

Figure 9. Effect of extractant concentration on the overall mass transfer coefficient.

10^{-5} cm·s^{-1} and D_{eff} was 23.40 × 10^{-7} cm·s^{-1}.the regression coefficient value of the performed modeling was R^2 = 0.9780.

3.5. Evaluation of Feed and Stripping Phase on the Permeability Coefficient

Applicability of HFSLM for separation of $^{152+154}$Eu from real acidic radioactive waste. The runs were made with real acidic waste. **Figure 11(a)** and **Figure 11(b)** shows that more than 82% of $^{152+154}$Eu was transported in receiving phase by recycle mode operation within 50 - 60 min, after 90 min the transported of $^{152+154}$Eu at 95.7% and raffinate of ^{90}Sr maintaining flow rate of 3 cm·s^{-1}, Re-maining $^{152+154}$Eu could be recovered by using fresh strippant or increasing the duration of the run.

4. Conclusion

The recovery of $^{152+154}$Eu and ^{90}Sr by hollow fiber liquid membrane afforded more than 97.7% for $^{152+154}$Eu and 50% for ^{90}Sr after 90 min when flow rate of feed was maintained 2 ml·min^{-1}. Selective permeation of $^{152+154}$Eu

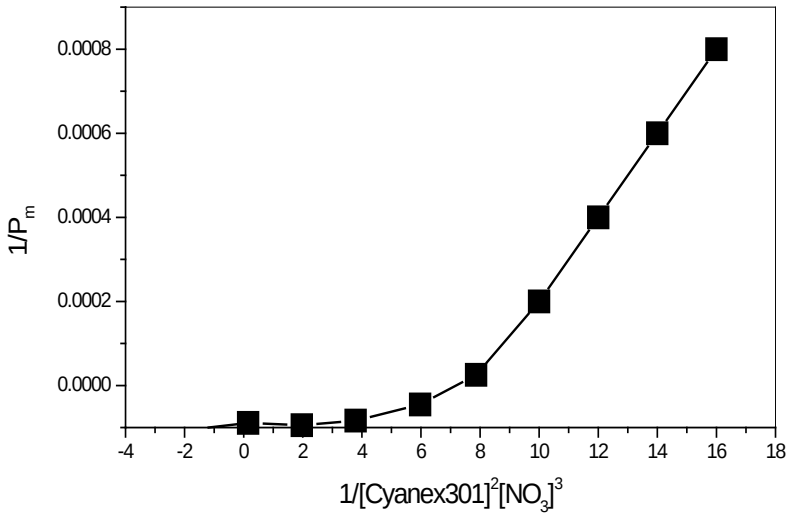

Figure 10. The slope of the straight line.

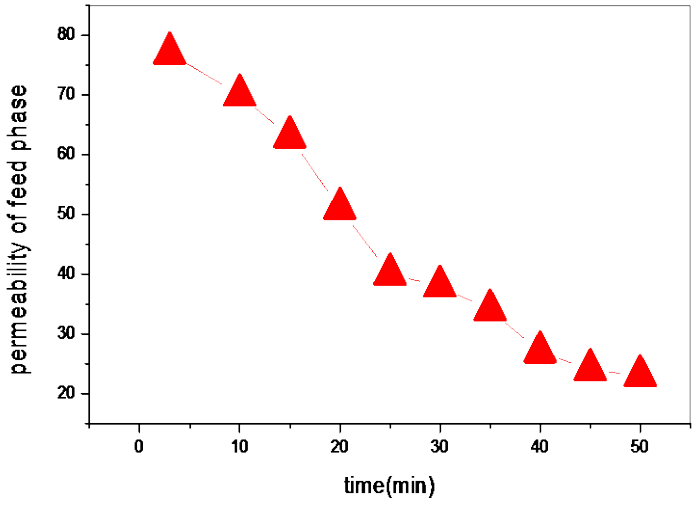

(a)

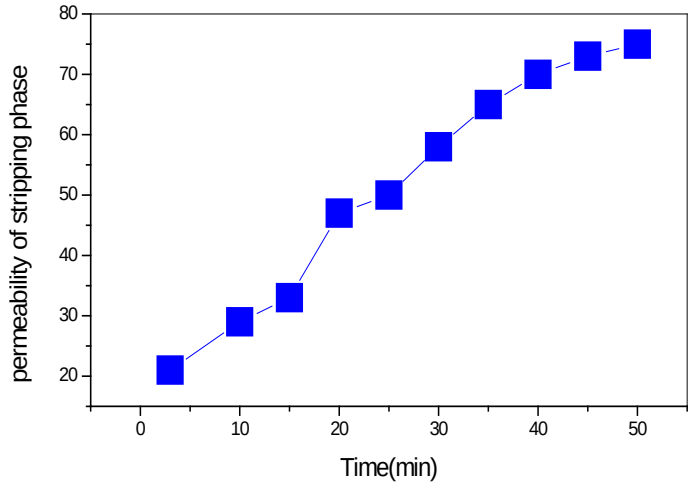

(b)

Figure 11. (a) Effect of feed phase on flow rate; (b) effect of stripping phase on flow rate.

and ^{90}Sr is clearly demonstrated from simulated waste solutions containing other fission products such as Ru^{106}, Cs137. It is possible to achieve an efficient separation of $^{152+154}Eu$ and ^{90}Sr presence of fission products rom nitate medium. The effect of carrier Cyanex/kerosene was achieve four times for $^{152+154}Eu$ than ^{90}Sr. The modeling of the effect of carrier was found in good agreement with results. The stability and reproducibility of the hollow fiber membrane were found to the best method in the impregnation mode. This is advantage in hollow fiber supported liquid membrane system to treat real and simulated waste streams for recovery of $^{152+154}Eu$ and ^{90}Sr from acidic waste.

References

[1] Arpa, C., Basyilmaz, E., Bektas, S., Genç, O. and Yurum, Y. (2000) Removal of Hg, Cd and Pb from Waste Water. *Fuel Processing Technology*, **68**, 111-120. http://dx.doi.org/10.1016/S0378-3820(00)00126-0

[2] Bringas, E., San Román, M.F., Irabien, J.A. and Ortiz, I. (2009) An Overview of the Mathematical Modelling of Liquid Membrane Separation Processes in Hollow Fiber Contactors. *Journal of Chemical Technology and Biotechnology*, **84**, 1583-1614. http://dx.doi.org/10.1002/jctb.2231

[3] Chakrabarty, K., Saha, P. and Ghoshal, A.K. (2010) Simultaneous Separation of Mercury and Lignosulfonate from Aqueous Solution Using Supported Liquid Membrane. *Journal of Membrane Science*, **346**, 37-44. http://dx.doi.org/10.1016/j.memsci.2009.09.010

[4] Vesa-Pekka Vartti, STUK - Radiation and Nuclear Safety Authority, Finland Baltic Sea Environment Fact Sheet 2013.

[5] Suter, T., Reyes-Suter, P., Gustafsson, S. and Marklund, I. (1962) Electromagnetic Transition Probabilities in Odd-A Mercury Isotope. *Nuclear Physics*, **29**, 33-65.

[6] Smith, K.L., Babcock, W.C., Baker, R.W. and Conrod, M.G. (1981) Coupled Removal of Chromium from Electroplating Rinse Solutions. In: *Chemistry in Water Reuse*, Ann Arbor Science Publishers, Ann Arbor, Mich., chap. 14.

[7] Shanghai Liquapure Filtation Co., Ltd. RM1301, 64, NO.555 HEXIA ROAD, JIADING SHANGHAI, SHANGHAI 201803 China.

[8] Zhao, L. Riensche, E. Menzer R., Blum, L. and Stolten. D. (2008) A Parametric Study of CO_2/N_2 Gas Separation Membrane Processes for Post-Combustion Capture. *Journal of Membrane Science*, **325**, 284-294. http://dx.doi.org/10.1016/j.memsci.2008.07.058

[9] Marcus, Y and Sen Gupta, A. (2001) Anil Kumar Pabby and Ana-Maria Sastre. *Ion Exchange and Solvent Extraction* (2001) *Marcel Dekker*, **15**, 331.

[10] David, J. and Herzog. H. (2000) The Cost of Carbon Capture. *Proceedings of the Fifth International Conference on Greenhouse Gas Control Technologies*, Cairns, 973-978.

[11] Singh, P. and Versteeg, G.F. (2008) Structure and Activity Relationships for CO_2 Regeneration from Aqueous Amine-Based Absorbents. *Process Safety and Environmental Protection*, **86**, 347-359. http://dx.doi.org/10.1016/j.psep.2008.03.005

[12] Gabelman, A. and Hwang, S.T. (1999) Hollow Fiber Membrane Contactors. *Journal of Membrane Science*, **159**, 61-106. http://dx.doi.org/10.1016/S0376-7388(99)00040-X

[13] Feron, P.H.M. and Jansen, A.E. (1995) Capture of Carbon Dioxide Using Membrane Gas Absorption and Reuse in the Horticultural Industry. *Energy Conversion and Management*, **36**, 411-414. http://dx.doi.org/10.1016/0196-8904(95)00032-9

[14] Klaassen, R., Feron, P.H.M. and Jansen, A.E. (2005) Membrane Contactors in Industrial Applications. *Chemical Engineering Research and Design*, **83**, 234-246. http://dx.doi.org/10.1205/cherd.04196

[15] Rangwala, H.A. (1996) Absorption of Carbon Dioxide into Aqueous Solutions Using Hollow Fiber Membrane Contactors. *Journal of Membrane Science*, **112**, 229-240. http://dx.doi.org/10.1016/0376-7388(95)00293-6

[16] Li, J.L. and Chen, B.H. (2005) Review of CO_2 Absorption Using Chemical Solvents in Hollow Fiber Membrane Contactors. *Separation and Purification Technology*, **41**, 109-122. http://dx.doi.org/10.1016/j.seppur.2004.09.008

[17] Fournier, R.L. (2007) Basic Transport Phenomena in Biomedical Engineering. Taylor & Francis, New York, 220.

[18] Sawicki, E. and Stróżyk, J. (2009) Determination of Permeability Coefficient. *Studia Geotechnica et Mechanica*, **31**.

[19] Kolthoff, I.M., Sandell, E.B., Meehan, E.J. and Bruckenstein, S. (1969) Quantitative Chemical Analysis. Macmillan, New York, 353.

[20] Alonso, A.I., Urtiaga, A. and Irabien, A. (1994) Inmaculada Ortiz, Extraction of Cr(VI) with Aliquat 336 in Hollow Fiber Contactors. *Chemical Engineering Science*, **49**, 901-909.

[21] Ergas, S.J. and Reuss, A.F. (2001) Hydrogenotrophic Denitrification of Drinking Water Using a Hollow Fibre Mem-

brane Bioreactor. *Journal of Water Supply*: *Research and Technology—AQUA*, **50**, 161-171.

[22] Ahmed, T. and Semmens, M.J. (1992) Use of Sealed End Hollow Fibers for Bubbleless Membrane Aeration: Experimental Studies. *Journal of Membrane Science*, **69**, 1-10. http://dx.doi.org/10.1016/0376-7388(92)80162-d

[23] Wongsawa, T., Pancharoen, U. and Lothongkum, A.W. (2013) World Academy of Science, Engineering and Technology. *International Journal of Chemical, Nuclear, Metallurgical and Materials Engineering*, **7**, 180-189.

Nomenclature

R^2: regression coefficient value
K_{ex}: extraction constant for tracer radioactive
Q_f: Total flow rate of feed solution
V_f: effective area of membrane and volume of the feed respectively
$P_{Eu,Sr}$: permeability coefficient of the tracer radioactive
N: number of fiber in module
L: length of fiber (cm)
r_i: internal radius of hollow fiber (cm)
r_{im}: mean radius (cm)
k_i, k_s: aqeous feed and aqeous stripping mass transfer coefficient ($cm \cdot s^{-1}$)
D_r: partition coefficient of radioactive flux ($mol \cdot cm^{-2} \cdot s^{-1}$)
K_m: membrane mass transfer coefficient
D_{eff}: diffusion coefficient
A: total internal area of hollow fiber module
V: total volume of feed
C_0: concentration of metal species solution
τ: tortuosity of membrane module
ε: porosity of hollow fiber module
d_{org}: membrane thickness boundry layer (cm)
T: absolute temperature
η: viscosity of membrane phase